BSS BASED I/Q IMBALANCE COMPENSATION IN COMMUNICATION RECEIVERS IN THE PRESENCE OF SYMBOL TIMING ERRORS

Mikko Valkama and Markku Renfors

Telecommunications Laboratory
Tampere University of Technology
P.O. Box 553, FIN-33101 Tampere, Finland

Visa Koivunen

Signal Processing Laboratory
Helsinki University of Technology
P.O. Box 3000, FIN-02015 HUT, Finland

ABSTRACT

In I/Q processing receivers, matching the amplitudes and phases of the I- and Q-branches is of major concern. In practise, matching can never be perfect in the analog front-end which results in insufficient rejection of the image frequency band. As a consequence, the desired channel signal is interfered by up to 50-100 dB stronger image signal and some kind of imbalance compensation is needed. In this paper, the interference due to imbalancing is modelled by instantaneous linear mixing model and the compensation is carried out by a blind source separation (BSS) method. The effects of symbol timing errors on EASI algorithm based compensation structure are analyzed both analytically and through computer simulations. The obtained results indicate that timing errors degrade the performance of the proposed method. The effects of timing errors can, however, be reduced with proper selection of non-linearity in the EASI algorithm.

1. INTRODUCTION

The principle of I/Q signal processing is widely utilized in all kinds of communication transceivers. Especially in the receiver side, the use of I/Q processing can simplify the receiver implementation considerably. For example, the so called low-IF and direct-conversion architectures both use I/Q downconversion to demodulate the signal from RF frequencies closer to baseband [1][2].

When the I- and Q-branches are perfectly matched, the image signal band is completely attenuated by the I/Q processing [1]. In practical implementations, however, the matching of the I- and Q-branches can never be perfect [1][2]. As a consequence, the image band rejection provided by the I/Q processing is finite and the desired channel signal is interfered by the image signal. With current analog circuit design, phase imbalance of 1-2° and amplitude imbalance of 1-2% are realistic resulting in 30-40 dB attenuation of the image signal [1][2].

This work was carried out in the project "Analog and Digital Signal Processing Techniques for Highly Integrated Transceivers" supported by the Academy of Finland.

In receiver structures using non-zero IF frequency, the image signal can be originally up to 50-100 dB stronger than the desired signal. This being the case, the attenuation provided by the I/Q processing alone is clearly insufficient and some kind of compensation is needed. Both analog and digital compensation techniques have been presented in the literature, see, e.g., [1]-[8]. In this paper, we propose a BSS based method for I/Q imbalance compensation. The problem is modelled as linear instantaneous mixing system and equivariant EASI [9] algorithm is employed in cancelling the interference. The method provides sufficient compensation behaviour with very few assumptions. It is expected, however, that symbol timing errors degrade the compensation performance. For this reason, the effects of timing errors on EASI algorithm based compensation structure are analyzed in detail. Eventhough the approach here is application specific, the results are directly applicable for analysing the effects of timing errors and other linear transformations on EASI algorithm in any source separation problem.

The paper is organized as follows. Section 2 presents the baseband signal model for analysing the imbalance effects. Also, the concept of blind source separation based imbalance compensation is considered. In Section 3, theoretical analysis of the effects of symbol timing errors on EASI algorithm based compensation structure is carried out. In Section 4, simulation results are provided to verify the theoretical analysis and conclusions are drawn in Section 5.

2. EASI ALGORITHM BASED IMBALANCE COMPENSATION

2.1 The Basic Signal Model

For the purpose of analysis, we model the whole imbalance between the I- and Q-branches as an imbalanced quadrature mixer [3] with local oscillator (LO) signal $x_{LO}(t) = \cos(\omega_{LO}t) - jg\sin(\omega_{LO}t + \phi)$, where g and ϕ represent the amplitude and phase imbalances, respectively. The local oscillator signal can also be written as

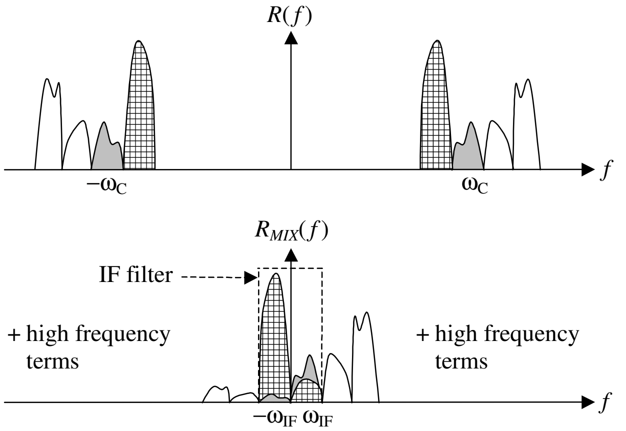

Figure 1. A frequency-domain illustration of the effects of I/Q imbalance. The desired channel signal (grey) is strongly interfered by the image signal (cross-hatched).

$$x_{LO}(t) = K_1 e^{-j\omega_{LO}t} + K_2 e^{j\omega_{LO}t}, \quad (1)$$

where the imbalance coefficients K_1 and K_2 are given by

$$K_1 = (1 + ge^{-j\phi})/2 \text{ and } K_2 = (1 - ge^{j\phi})/2. \quad (2)$$

As a model, the received signal $r(t)$ is quadrature mixed with the local oscillator signal $x_{LO}(t)$. Due to imbalances, K_2 is not identical to zero and two frequency translations instead of one will take place. This results in a mixer output signal $r_{MIX}(t)$ where the image signal appears as interference on top of the desired signal. This effect is illustrated in frequency-domain in Fig. 1 where the IF frequency ω_{IF} is selected to be half of the channel spacing.

To compensate the effects of imbalance, signal components around both the negative and positive IF frequencies can be used [3][4]. This results in two baseband observations $d(n)$ and $v(n)$ of the form

$$d(n) = K_1 s(n) + K_2 i^*(n), \quad (3)$$

$$v(n) = K_2^* s(n) + K_1^* i^*(n), \quad (4)$$

where $s(n)$ and $i(n)$ are the baseband equivalent desired channel and image band signals, respectively. For a detailed derivation and motivation for the signals in Eqs. (3) and (4), see [3][4].

2.2 Source Separation Based Compensation

Assuming that the receiver imbalance properties do not depend on frequency, the imbalance coefficients K_1 and K_2 in Eq. (2) are also frequency independent. Then, the effects of imbalances can be modelled as instantaneous signal mixtures as given by Eqs. (3) and (4). Furthermore, $s(n)$ and $i(n)$ can be assumed to be mutually independent and a blind source separation algorithm operating on $d(n)$ and $v(n)$ can be used for imbalance compensation.

To fit the signal model of Eqs. (3) and (4) into the general source separation formulation, we can write it in terms of unit variance source signals as

$$\mathbf{x}(n) = \mathbf{A}\mathbf{s}(n), \quad (5)$$

where

$$\mathbf{x}(n) = \begin{bmatrix} d(n) & v(n) \end{bmatrix}^T \text{ and } \mathbf{s}(n) = \begin{bmatrix} s_1(n) & s_2(n) \end{bmatrix}^T. \quad (6)$$

The unit variance source signals $s_1(n)$ and $s_2(n)$ of Eq. (6) are given by

$$s_1(n) = s(n)/\sqrt{P_S} \text{ and } s_2(n) = i^*(n)/\sqrt{P_I}, \quad (7)$$

where $P_X = E(|x(n)|^2)$ denotes the power of $x(n)$, in general. This notation is used throughout this paper. The mixing matrix $\mathbf{A}$ in Eq. (5) is then given by

$$\mathbf{A} = \begin{bmatrix} K_1\sqrt{P_S} & K_2\sqrt{P_I} \\ K_2^*\sqrt{P_S} & K_1^*\sqrt{P_I} \end{bmatrix}. \quad (8)$$

Given the observation vector $\mathbf{x}(n)$, adaptive estimation of the source signals $s_1(n)$ and $s_2(n)$ of Eq. (7) is in general given by another matrix multiplication as

$$\begin{aligned} \mathbf{y}(n) &= \mathbf{B}(n)\mathbf{x}(n) \\ &= \mathbf{C}(n)\mathbf{s}(n), \end{aligned} \quad (9)$$

where the total equivalent system $\mathbf{C}(n) = \mathbf{B}(n)\mathbf{A}$. Since the sources are usually assumed to be statistically independent, the separating matrix $\mathbf{B}(n)$ can be adapted to minimize a measure of mutual dependence between the separator output signals [9]-[12].

The family of EASI algorithms [9][10] update the separating matrix $\mathbf{B}(n)$ of Eq. (9) serially as

$$\mathbf{B}(n+1) = \left(\mathbf{I} - \lambda(n)\mathbf{H}(\mathbf{y}(n))\right)\mathbf{B}(n), \quad (10)$$

where $\lambda(n)$ is the adaptation step-size. The matrix-valued function $\mathbf{H}(.)$ in Eq. (10) is of the form

$$\mathbf{H}(\mathbf{y}) = \mathbf{y}\mathbf{y}^H - \mathbf{I} + \mathbf{f}(\mathbf{y})\mathbf{y}^H - \mathbf{y}\mathbf{f}(\mathbf{y})^H, \quad (11)$$

where $\mathbf{f}(.)$ is any non-linear function operating component-wise on its argument. In general, the separation performance of the EASI algorithms is independent of the actual mixing matrix [9][10]. This is usually referred to as the equivariance property.

2.3 Receiver Structure

A generalized receiver structure utilizing the concept of source separation based imbalance compensation is presented in Fig. 2. In order to generate the needed observations $d(n)$ and $v(n)$ for the separation algorithm, the sampled IF signal is divided into two branches and signal components around both the negative and positive IF frequencies are used. The general sampling rate requirements are defined by the selected IF frequency. After the digital FIR filters of Fig. 2, decimation to symbol rate samples is, however, always possible. With proper selection of IF frequency, the image band signal is also another signal band and two actual user signals can be estimated as $y_1(n)$ and $y_2^*(n)$.

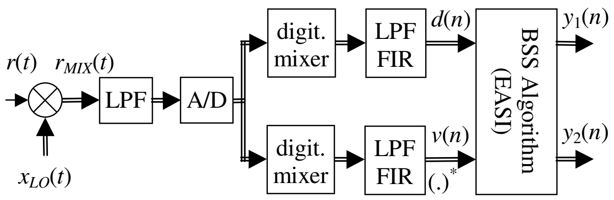

Figure 2. A simplified block-diagram of the blind source separation based I/Q imbalance compensation scheme.

3. SYMBOL TIMING ERROR ANALYSIS

3.1 Performance Measure

The separation performance is usully measured in terms of signal-to-interference ratios (SIR) at the separator output signals. Based on Eq. (9) and the assumption of unit-variance source signals, these can now be defined as

$$SIR_{ij} = \frac{E(|C_{ii}|^2)}{E(|C_{ij}|^2)}. \tag{12}$$

With realistic adaptation step-size, the steady-state value of $E(|C_{ii}|^2)$ is practically equal to unity. This leads to the definition used in [9].

The general performance analysis for the EASI algorithm is given in [9]. For convenience, the steady-state solution is reproduced here as

$$SIR_{ij} = \lambda^{-1}\left(\frac{1}{4} + \frac{1}{2}\frac{\gamma_i + \gamma_j}{\kappa_i + \kappa_j} + \beta_{ij}^{+} + \beta_{ij}^{-}\right)^{-1}, \tag{13}$$

where

$$\beta_{ij}^{+} = \frac{2(\kappa_i + \kappa_j)(\mu_i - \mu_j)^2 + (\kappa_i - \kappa_j)^2}{4(\kappa_i + \kappa_j)(2 + \kappa_i + \kappa_j)}, \tag{14}$$

$$\beta_{ij}^{-} = \frac{(2\mu_i - \kappa_i) - (2\mu_j - \kappa_j)}{2(2 + \kappa_i + \kappa_j)}. \tag{15}$$

The non-linear moments κ_i, μ_i and γ_i in Eqs. (13)-(15) depend on the original source distibutions as well as on the non-linear functions $f_i(y_i)$ used in the adaptation. Clearly, Eq. (13) presents a performance bound of $4/\lambda$ for identical source distributions. For simplicity, we assume that a simple cubic non-linearity [9][11] of the form $f_i(y_i) = y_i|y_i|^2$ is used henceforth. Then, the non-linear moments κ_i, μ_i and γ_i can be written as [5][9]

$$\kappa_i = 2 - E(|s_i|^4), \tag{16}$$

$$\gamma_i = E(|s_i|^6) - (E(|s_i|^4))^2, \tag{17}$$

$$\mu_i = E(|s_i|^4). \tag{18}$$

Assuming ideal symbol rate sampling and QPSK sources, it was demonstrated in [5] that the upper bound of $4/\lambda$ can be reached using the given cubic non-linearity. This, however, is not the case in the presence of timing errors.

3.2 Linear Model for Timing Errors

A linearly modulated communication signal $X(t)$ corresponding to a symbol sequence $x(n)$ is in general given by

$$X(t) = \sum_k x(k)p(t - kT), \tag{19}$$

where T denotes the symbol interval and $p(t)$ is the total equivalent pulse-shape representing the effects of the transmit and receive filters and the channel [13]. Then, symbol rate sampling with timing error τ yields

$$\begin{aligned} \tilde{x}(n) &= X(nT + \tau) \\ &= \sum_k x(k)\bar{p}(n - k), \end{aligned} \tag{20}$$

where $\bar{p}(n) = p(nT + \tau)$. Based on this, the effective source signals for the desired user and the interferer with timing errors τ_1 and τ_2, respectively, are now given by

$$\tilde{s}(n) = \sum_k s(k)\bar{p}_1(n - k), \tag{21}$$

$$\tilde{i}(n) = \sum_k i(k)\bar{p}_2(n - k), \tag{22}$$

where $\bar{p}_i(n) = p_i(nT + \tau_i)$, i = 1, 2. Then, the effective baseband equivalent model can be written as

$$\tilde{d}(n) = K_1\tilde{s}(n) + K_2\tilde{i}^*(n), \tag{23}$$

$$\tilde{v}(n) = K_2^*\tilde{s}(n) + K_1^*\tilde{i}^*(n). \tag{24}$$

Assuming that the desired user and interferer symbol streams $s(n)$ and $i(n)$ are i.i.d. sequences, the powers of $\tilde{s}(n)$ and $\tilde{i}(n)$ are given by

$$E(|\tilde{s}(n)|^2) = G_1P_S, \tag{25}$$

$$E(|\tilde{i}(n)|^2) = G_2P_I, \tag{26}$$

where $G_i = \sum_k \left| \bar{p}_i(k) \right|^2$, i = 1, 2. Then, the corresponding unit variance source signals can be written as

$$\tilde{s}_i(n) = \sum_k s_i(k)\tilde{p}_i(n-k), \tag{27}$$

where $\tilde{p}_1(n) = \bar{p}_1(n)/\sqrt{G_1}$, $\tilde{p}_2(n) = \bar{p}_2^*(n)/\sqrt{G_2}$ and $s_i(n)$ are given by Eq. (7), i = 1, 2. As a result, we can write the signal model of Eqs. (23) and (24) in terms of the effective unit variance source signals $\tilde{s}_1(n)$ and $\tilde{s}_2(n)$ as

$$\begin{bmatrix} \tilde{d}(n) \\ \tilde{v}(n) \end{bmatrix} = \begin{bmatrix} K_1\sqrt{G_1 P_S} & K_2\sqrt{G_2 P_I} \\ K_2^*\sqrt{G_1 P_S} & K_1^*\sqrt{G_2 P_I} \end{bmatrix} \begin{bmatrix} \tilde{s}_1(n) \\ \tilde{s}_2(n) \end{bmatrix}. \tag{28}$$

3.3 Statistical Analysis

To analyze the effects of timing errors, we first obtain a proper statistical characterization in terms of fourth and sixth order moments of the source signals of Eq. (28). In the analysis, unit variance symbol sequences $s_1(n)$ and $s_2(n)$ are assumed to be QPSK modulated, zero mean, i.i.d. sequences that are independent of each other. Also, all the symbols are assumed to be equally probable, so

$$E(s_i^2) = E(s_i^3) = E(\left|s_i\right|^2 s_i) = 0. \tag{29}$$

Based on Eq. (27), the above circularity properties hold also for the effective source signals $\tilde{s}_i(n)$. Using the well-known moment-to-cumulant formula [14], the fourth order cumulant $\tilde{C}_{4,i}$ of $\tilde{s}_i(n)$ can then be written at zero lag as

$$\begin{aligned} \tilde{C}_{4,i} &= E(\left|\tilde{s}_i(n)\right|^4) - 2(E(\left|\tilde{s}_i(n)\right|^2))^2 \\ &= E(\left|\tilde{s}_i(n)\right|^4) - 2 \end{aligned} \tag{30}$$

As a result of Eq. (27), $\tilde{C}_{4,i}$ can also be written as

$$\tilde{C}_{4,i} = C_{4,i}\sum_k \left|\tilde{p}_i(k)\right|^4 = -\sum_k \left|\tilde{p}_i(k)\right|^4, \tag{31}$$

where $C_{4,i} = -1$ is the fourth order cumulant of $s_i(n)$ at zero lag [14]. Eqs. (30) and (31) can then be solved for the fourth order moment of $\tilde{s}_i(n)$ to yield

$$E(\left|\tilde{s}_i(n)\right|^4) = 2 - \sum_k \left|\tilde{p}_i(k)\right|^4. \tag{32}$$

To derive an expression for the corresponding sixth order moment of $\tilde{s}_i(n)$, we can again utilize the moment-to-cumulant formula combined with the circularity properties and write the sixth order cumulant $\tilde{C}_{6,i}$ at zero lag as

$$\begin{aligned} \tilde{C}_{6,i} &= E(\left|\tilde{s}_i(n)\right|^6) - 9E(\left|\tilde{s}_i(n)\right|^2)E(\left|\tilde{s}_i(n)\right|^4) \\ &\quad + 12(E(\left|\tilde{s}_i(n)\right|^2))^3. \end{aligned} \tag{33}$$

The result of Eq. (33) can be simplified to yield

$$\tilde{C}_{6,i} = E(\left|\tilde{s}_i(n)\right|^6) - 9E(\left|\tilde{s}_i(n)\right|^4) + 12. \tag{34}$$

Based on Eq. (27), $\tilde{C}_{6,i}$ can also be written as

$$\tilde{C}_{6,i} = C_{6,i}\sum_k \left|\tilde{p}_i(k)\right|^6 = 4\sum_k \left|\tilde{p}_i(k)\right|^6, \tag{35}$$

where $C_{6,i} = 4$ is the sixth order cumulant of $s_i(n)$ at zero lag. Then, we can combine the results of Eqs. (32)-(35) and write the sixth order moment of $\tilde{s}_i(n)$ as

$$E(\left|\tilde{s}_i(n)\right|^6) = 4\sum_k \left|\tilde{p}_i(k)\right|^6 + 6 - 9\sum_k \left|\tilde{p}_i(k)\right|^4. \tag{36}$$

Finally, the results of Eqs. (32) and (36) can be used to calculate the moments of Eqs. (16)-(18) for $\tilde{s}_i(n)$, and further, to evaluate the effects of timing errors on the separation performance. Eventhough the analysis was carried out for QPSK signals, the previous calculations are generic in the sense that only the values of $C_{4,i}$ and $C_{6,i}$ are modulation specific. For example, the results are as such directly applicable to any complex PSK signals and with minor modifications, also to the complex QAM signals. Since the effects of also other linear transformations on the EASI algorithm can be analyzed in a similar manner as the timing errors, the results are of general importance. Numerical illustrations as well as results of example simulations are given in Section 4.

4. ANALYTICAL AND SIMULATED RESULTS

In the illustrations, QPSK modulation and raised-cosine pulse-shapes $p_i(t)$ are used with a typical roll-off factor of 0.35. The cubic non-linearity is used in most of the cases while also a more robust non-linear function is examined. In the simulations, imbalance values of g = 1.02 and ϕ = 2° are used representing a realistic analog front-end design. The original SIR defined as the power ratio P_S / P_I between the desired and image band signals ranges from an extremely difficult case of -80 dB to 0 dB. Values higher than those should be manageable with the image rejection provided by the I/Q processing alone. In order to achieve both fast adaptation and adequate steady-state SIR, the step-size λ is selected to be 0.02 for the first 1000 samples and 0.002 after that. The total number of samples used in the simulations is 3000. When needed, ensemble averaging is carried out through 100 independent trials.

The effects of timing errors on the steady-state SIR performance are illustrated in Fig. 3 from the desired user point of view. Clearly, the cubic non-linearity is sensitive to the desired signal's timing error τ_1. The maximum performance degradation is approximately 5 dB. The corresponding results of example simulations are presented in Fig. 4 with original SIR = −40 dB. Without any doubt, the simulation results agree with theory. Notice that the reference situation of ideal sampling studied in [5] is obtained from Fig. 3 with $\tau_1 = \tau_2 = 0$. It can be seen that sufficient image rejection is always obtained when $\tau_1 = 0$ regardless of the interferers timing error τ_2.

After successful separation of the desired and image channel signals, the effects of possible symbol timing errors on the individual user data streams are, as usually, corrected by symbol synchronization techniques. This, however, is out of the scope of this paper. As demonstrated by Fig. 3, the compensation performance is only slightly dependent on the interferer's timing error τ_2. Consequently, no synchronization between the individual users is needed. This is, of course, highly desirable from the whole communication system point of view.

The equivariance property of EASI algorithm is illustrated in Fig. 5. As can be seen, the separation performance is independent of the relative powers of the source signals, even in the presence of additive noise. For further illustration, one realizations of the total equivalent mixture coefficients C_{ij} are presented in Fig. 6 with original SIR = −40 dB. Since C_{11} and C_{12} (C_{22} and C_{21}) converge in absolute value to unity and zero, respectively, the recovery of $\tilde{s}_1(n)$ ($\tilde{s}_2(n)$) is successful.

To further reduce the effects of desired user's timing errors, a more robust non-linearity can be used. Motivated by the changes in the source statistics, a "hole puncher" -type of non-linear function of the form

$$f_i(y_i) = \begin{cases} -y_i & if \quad |y_i|^2 \le \alpha \\ 0 & otherwise \end{cases} \qquad (37)$$

is tested. The results of example simulations for $\alpha = 0.9$ are given in Table I with original SIR = −40 dB. Clearly, the proposed function is much more robust against the timing errors than the cubic non-linearity.

5. CONCLUSIONS

The principle of I/Q signal processing is vastly utilized in today's radio receivers. When the amplitudes and phases of the I- and Q-branches are perfectly matched, the use of I/Q processing completely attenuates the image band. In practise, however, imbalances cannot be avoided in the analog front-end and the image band signal appears as interference on top of the desired signal. Especially, in case of non-zero IF frequency, the interfering signal can be originally 50-100 dB stronger than the desired channel signal and some kind of compensation is needed.

Here, the effects of imbalances were modelled as instantaneous signal mixtures and EASI source separation algorithm based compensation was considered. Especially, the effects of timing errors and other possible linear transformations on the separation performance were evaluated both analytically and through computer simulations. As evidenced by the obtained results, the "standard" cubic non-linearity is sensitive to the desired signal's timing errors. With raised-cosine pulse-shapes, the maximum performance degradation was shown to be approximately 5 dB. With other kinds of linear transformations, the effects will be even more drastic. For certain applications, this can be unacceptable and some other non-linear function should be used. For this purpose, a more robust "hole puncher" -type of non-linearity was proposed and its efficiency was demonstrated by simulations.

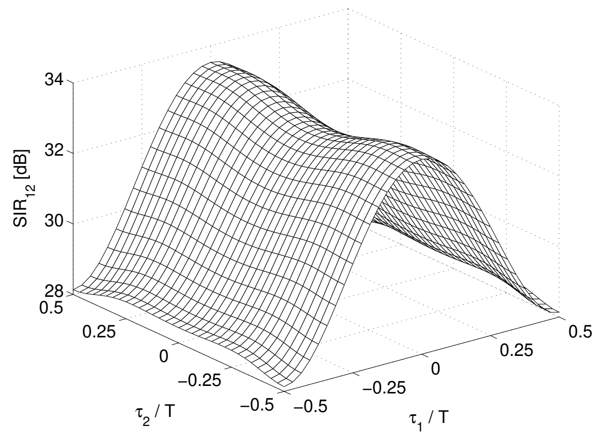

Figure 3. Theoretical SIR performance for the desired user as a function of timing errors τ_1 and τ_2. Adaptation step-size λ = 0.002, cubic non-linearity.

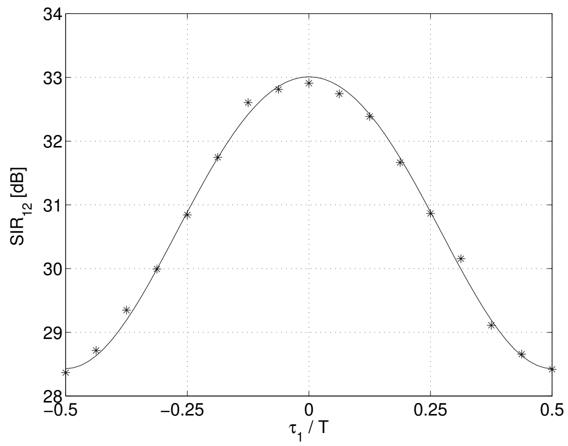

Figure 4. Theoretical (solid) and simulated (star-marked) SIR performance for the desired user as a function of timing error τ_1. Interfering signal is ideally sampled (τ_2 = 0). Adaptation step-size λ = 0.002 (theoretical), 0.02-0.002 (simulations), cubic non-linearity, no noise.

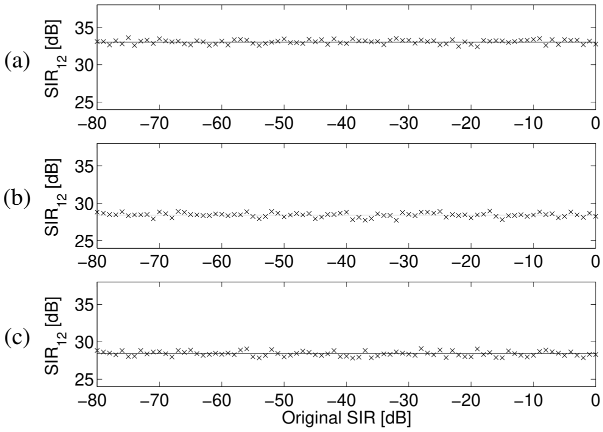

Figure 5. Theoretical (solid) and simulated (x-marked) SIR performance for the desired user. (a): τ_1 = 0, no noise. (b): τ_1 = T/2, no noise. (c): τ_1 = T/2, SNR = 20 dB. Interfering signal is ideally sampled (τ_2 = 0). Adaptation step-size λ = 0.002 (theoretical), 0.02-0.002 (simulations), cubic non-linearity.

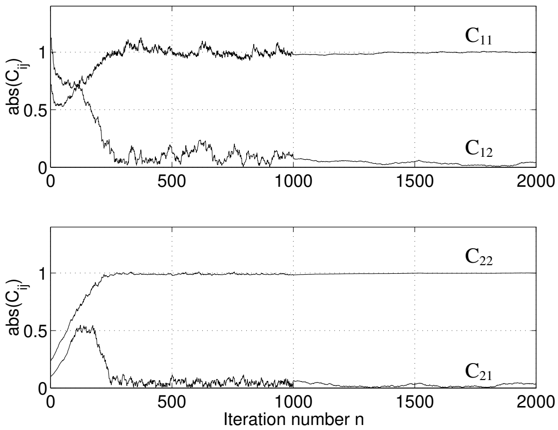

Figure 6. One realization of the total equivalent mixture coefficients C_{ij}. τ_1 = T/2, τ_2 = 0, SNR = 20 dB. Adaptation step-size λ = 0.02-0.002, cubic non-linearity.

TABLE I

Comparison of cubic and "hole puncher" non-linearities in terms of simulated steady-state SIR. Interfering signal is ideally sampled (τ_2 = 0). Adaptation step-size λ = 0.02-0.002, no noise.

	SIR_{12} [dB]	
τ_1 / T	cubic	"hole puncher"
– 1/2	28.4	31.9
– 1/4	30.8	32.6
0	32.9	32.8
1/4	30.9	32.5
1/2	28.4	31.8

6. REFERENCES

[1] J. Crols and M. S. J. Steyaert, "Low-IF topologies for high-performance analog front ends of fully integrated receivers," *IEEE Trans. on Circuits and Systems-II*, vol. 45, pp. 269-282, March 1998.

[2] B. Razavi, "Architectures and circuits for RF CMOS receivers," in *Proc. IEEE Custom Integrated Circuits Conference*, Santa Clara, CA, USA, May 1998, pp. 393-400.

[3] M. Valkama, M. Renfors, and V. Koivunen, "Advanced methods for I/Q imbalance compensation," to be submitted to *IEEE Trans. on Signal Processing*.

[4] M. Valkama, M. Renfors, and V. Koivunen, "On the performance of interference canceller based I/Q imbalance compensation," to be presented in *IEEE Int. Conf. on Acoustics, Speech and Signal Processing*, Istanbul, Turkey, June 2000.

[5] M. Valkama, M. Renfors, and V. Koivunen, "Blind source separation based I/Q imbalance compensation," submitted to *IEEE Symposium* 2000 *on Adaptive Systems for Signal Processing*, *Communication and Control*, Lake Louise, Alberta, Canada, October 2000.

[6] J. K. Cavers and M. W. Liao, "Adaptive compensation for imbalance and offset losses in direct conversion transceivers," *IEEE Trans. on Vehicular Technology*, vol. 42, pp. 581-588, November 1993.

[7] J. P. F. Glas, "Digital I/Q imbalance compensation in a low-IF receiver," in *Proc. IEEE Globecom 98*, Sydney, Australia, November 1998, pp. 1461-1466.

[8] L. Yu and W. M. Snelgrove, "A novel adaptive mismatch cancellation system for quadrature IF radio receivers," *IEEE Trans. on Circuits and Systems-II*, vol. 46, pp. 789-801, June 1999.

[9] J.-F. Cardoso and B. H. Laheld, "Equivariant adaptive source separation," *IEEE Trans. on Signal Processing*, vol. 44, pp. 3017-3030, December 1996.

[10] J.-F. Cardoso, "Blind source separation: Statistical principles," *Proc. of the IEEE*, vol. 86, pp. 2009-2025, October 1998.

[11] S. Choi, A. Cichocki, and S. Amari, "Flexible independent component analysis," in *Proc. IEEE SP Society Workshop on Neural Networks for Signal Processing*, Cambridge, UK, August 1998, pp. 83-92.

[12] J. Karhunen, E. Oja, L. Wang, R. Vigário, and J. Joutsensalo, "A class of neural networks for independent component analysis," *IEEE Trans. on Neural Networks*, vol. 8, pp. 486-504, May 1997.

[13] E. A. Lee and D. G. Messerschmitt, *Digital Communication*, Kluwer Academic Publishers, Boston, 1988.

[14] J. M. Mendel, "Tutorial on higher-order statistics (spectra) in signal processing and system theory: Theoretical results and some applications," *Proc. of the IEEE*, vol. 79, pp. 278-305, March 1991.